Longitudinal Non-Destructive Characterization of Nested Antiresonant Nodeless Fiber Microstructure Geometry and Twist

Leonard Budd,[1,*] Austin Taranta,[1] Eric Numkam Fokoua,[1] and Francesco Poletti[1]

[1] *Optoelectronics Research Centre, University of Southampton, University Rd, Southampton SO17 1BJ, UK*

[*] *l.g.budd@soton.ac.uk*

Abstract: We demonstrate non-destructive measurement of nested antiresonant nodeless fiber (NANF) microstructure along 2.2 km of fiber using a side-scattering method. Additionally, using the same technique, we demonstrate measurement of twisting in NANF.

1. Introduction

Hollow core optical fibers (HCFs) are rapidly emerging as a compelling alternative to conventional fiber technology, offering the opportunity to overcome the intrinsic limitations associated with silica core fibers. Guiding light through a hollow core rather than bulk silica gives the potential for enhanced performance, including: lower loss, lower latency and reduced optical non-linearity. At the forefront of HCF technology is a class of antiresonant fiber with a microstructure consisting of multiple circular glass capillaries surrounding the central core. In particular, we will be focusing on the nested antiresonant nodeless fiber (NANF) [1], the first HCF to demonstrate loss lower than 1 dB/km [2], which was subsequently lowered to 0.22 dB/km at 1300 and 1625 nm [3]. A microscope image of a 5 nested element NANF cross-section is shown in Fig. 1a. The nested element adds an additional antiresonant reflecting layer, which acts to reduce the confinement loss of the fiber significantly. Also key to the fiber's operation is the size of the hollow cavity between the smaller inner and larger outer capillaries. If correctly sized, this can couple strongly to higher order modes in the fiber core, 'stripping' them away and leading to the effectively single-mode operation required in long-haul telecommunications [1]. It is therefore clear that, in order to achieve the desired operating parameters, careful control of this microstructure is needed along the fiber. During fabrication, this is currently achieved by cutting a fiber sample, viewing the microstructure under a microscope and making any necessary parameter adjustments. Not only is this highly time consuming, it greatly reduces the yield of a given fiber draw. There is also the chance that defects or drastic changes to the microstructure may occur between sampling points, meaning that the impaired performance of the fiber is not known until characterization. Hence, to draw long lengths of uniformly good fiber, it is highly desirable to have some method of non-destructively measuring the inner microstructure dimensions. Such a method could also be applied, in principle, to measure the rate and direction of microstructure twist along the length of fiber, something impossible to do in a circularly symmetric solid-core fiber. This would enable better control of the polarization properties of the fiber, and bring advantages to those applications which require the fiber to be bent into a coil. Here, the orientation of the microstructure with respect to the bend plane can cause variations in macrobending loss and bend-induced birefringence [4].

In this work, we use a side-scattering interferometric method first described in 2019 for tubular fibers (no nested elements) [5], and subsequently demonstrated at a single spatial location on a NANF [6], and double nested antiresonant nodeless fiber (DNANF) [7]. Using a similar setup mounted to two different rewinder systems, we demonstrate the non-destructive and longitudinally resolved measurement of both microstructure twist and capillary diameters in NANF.

2. Method

A schematic of the experiment is shown in Fig. 1b. A rewinder feeds the NANF through a measurement setup which probes the side of the fiber. This consists of a white light source (WLS) coupled into a multimode fiber (MM1) which is collimated by a lens (L) onto the side of the NANF. This light is scattered by the NANF, collected by a 600 μm core fiber (MM2) and fed into a high-resolution spectrometer with an integration time of 50 ms. Two different rewinders were used in this investigation. For probing fiber twist, we used an in-house rewinder which uses a motorized rotary stage to rotate the take-up spool and pull the fiber through the beam path of the WLS. Here, the fiber payout spool is held on a gimbal which allows the fiber to be rotated about its longitudinal axis. For longer lengths of fiber, we mounted the measurement setup in the fiber path of a commercially-available rewinder. In both instances, the rewinder is connected to a computer which reads its position and synchronizes this with the associated spectrometer reading. A portion of the light incident on the fiber enters into and makes a round trip through one of the fiber capillaries, whereas some of the light simply reflects off the air-glass interface between the fiber jacket and hollow core. We see the interaction between these

optical paths as an interference pattern in the spectral domain. A Fourier transform of the collected spectra yields peaks in the time domain corresponding to the time difference between the optical paths. For NANF, as theoretically predicted [5], and subsequently experimentally demonstrated [6], we see peaks for each of the two nested capillaries, as well as a signal corresponding to the difference in the two capillary diameters. An additional predicted sum signal is unresolvable due to the spectrometer resolution. We map the temporal position of these peaks to capillary diameters using a geometrical optics model first outlined in [6], which calculates all the relevant optical path lengths as a function of fiber geometry.

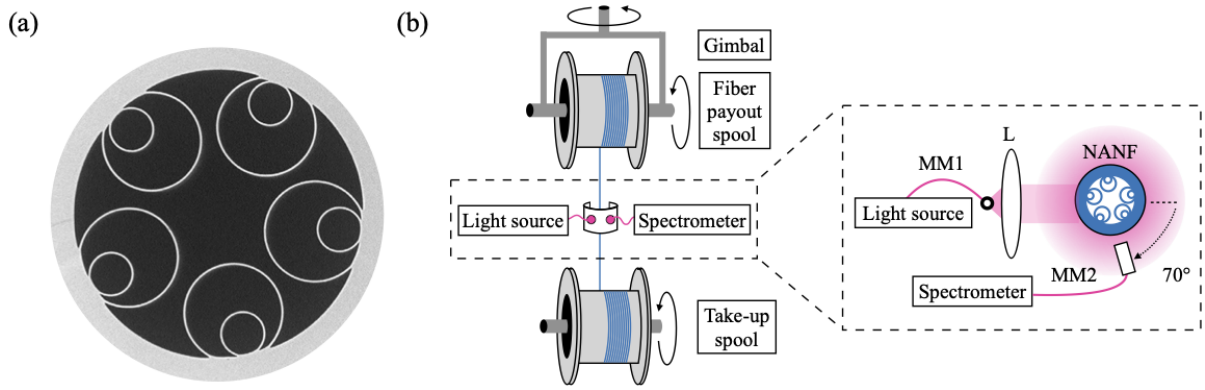

Fig. 1: (a) SEM cross-section of a 5-capillary NANF. Light propagates in the 25 μm diameter central core where it is confined by 5 concentric pairs of circular glass capillaries. (b) Experimental setup schematic showing fiber rewinder and measurement system.

3. Results

Fig. 2 shows a non-destructive measurement of twisting in NANF. We make a surface plot of the collected time domain power as a function of fiber length and capillary diameter (Fig. 2a). From this we can see that there are discrete periodic regions of increased power at locations corresponding to the diameters of the inner and outer NANF capillaries. The longitudinal separation between signals arises from the beam being incident on the gap between capillaries as the fiber twists. This leads to oscillations in the maximum collected power along the length. By determining the locations at which this signal is maximum, we obtain the position of each capillary (Fig. 2b). We consider the maximum power in the region corresponding to 10-20 μm as the signal from the inner capillaries is, in general, more powerful than that of the outer capillaries. Dividing the number of detected capillary signals by the total number of capillaries in the fiber (5 in this case) allows one to infer the total number of rotations imparted to the fiber. We apply successive manual rotations to the fiber using the gimbal and measure the total fiber twist by counting the number of different capillaries detected by the measurement setup as the fiber is wound through. For each of the 4 gimbal rotations, we collect data along 5 meters of fiber with a longitudinal resolution of 0.07 mm. We can see that, as expected, rotating the gimbal does indeed increase the number of detected capillaries along a given length of fiber (Fig. 2c). Each full rotation of the gimbal leads to a mean of 1.17 additional detected fiber rotations (around 6 extra capillaries in the first 5 m). This marginally higher than expected twist rate may arise due to uncontrolled twist introduced between measurements, when the fiber is rewound to the original payoff spool.

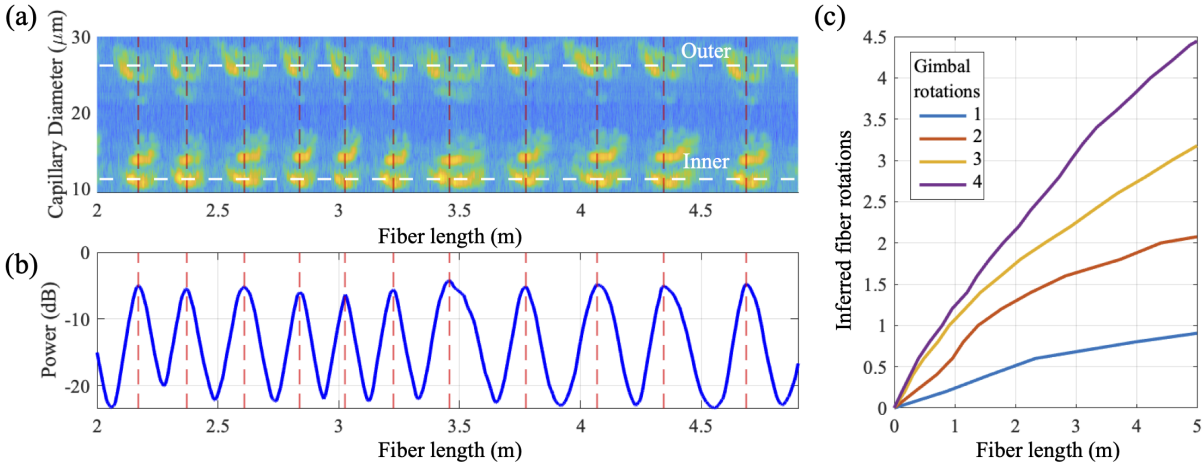

Fig. 2: Fiber twisting results. (a) Surface plot from fiber with 4 gimbal rotations applied, showing signals from inner and outer NANF capillaries at 11 μm and 25 μm respectively (white horizontal dashed lines). Also note the signals corresponding to the difference in the two capillary diameters at 14 μm. (b) Maximum power from above surface plot in the 10-20 μm region, used to obtain the capillary positions. (c) Measured total fiber rotations for successive gimbal rotations.

We can also use this method to measure the variation in capillary diameter along the length of the fiber. To demonstrate this, we pass a 2.2 km sample of NANF through the setup, collecting side-scattering spectra along the fiber length. To verify the consistency of the technique, we take three sets of data: two at a slow rewinder speed (4.2 m/min, longitudinal resolution of 1.3 cm) along opposite directions of the fiber, and one at approximately 9 times the speed (36 m/min, longitudinal resolution of 14 cm). These results are overlaid in Fig. 3 below. We analyze this data in a manner similar to the prior experiment: the maximum power for the time bin which encompasses the inner capillaries is extracted and tracked over the fiber length. From this curve, the local maxima are used as reference points at which the capillary diameters are computed, and the result is plotted in Fig. 3 giving a 25 m (approximately 5 full fiber rotations), moving average and standard deviation for each set of capillaries (inner and outer). The mean inner and outer capillary measurements at the start and end of the fiber measured using a microscope are shown in black at 0 and 2.2 km.

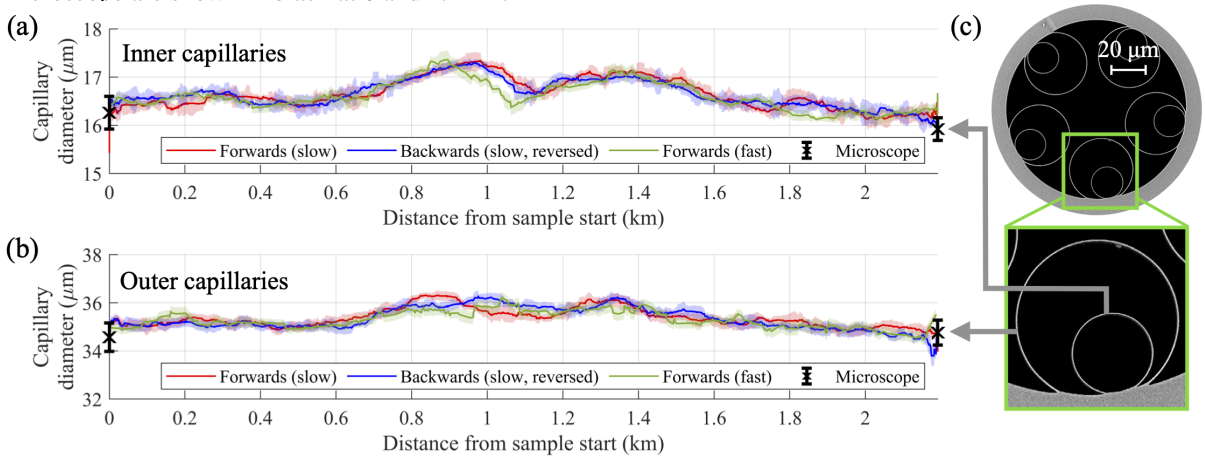

Fig. 3: Non-destructive measurement of inner (a) and outer (b) capillary diameters along 2.2 km of NANF. Solid traces and shaded regions show the 25 m moving average and standard deviation respectively. The blue and red traces were taken along opposite directions of the fiber at a rewinder speed of 4 m/min, with the *x*-axis of the blue trace reversed. The green trace was taken along the forwards direction at a rewinder speed of 36 m/min. The black points are optical microscope measurements of the mean capillary diameters at each end of the sample; the error bars depict the maximum and minimum diameters. (c) SEM image of fiber cross section showing inner and outer nested capillaries.

There is good agreement between all measurements, with less than 0.05 μm mean difference for all the inner and outer capillary measurements. The microscope measures mean inner diameters of 16.26 and 15.92 μm at either end of the fiber sample, a 2.1% change which suggests relative uniformity along the length. However, the non-destructive measurement allows us to observe considerable variation in capillary diameters, which increases to as high as 17.3 μm at the 0.9km position, an increase of 6.4%. This pattern is also seen for the outer capillary measurements, where there is only a 0.19 μm (0.5%) difference between the 34.57 μm and 34.76 μm microscope measurements at the beginning and end of the sample respectively. Again at around 0.9 km in length, the diameter in fact becomes as large as 36.1 μm, a 4.4% increase. Similarly to the inner capillaries, another increase is seen at around 1.3 km, suggesting a variation in the fabrication parameters around this point.

4. Conclusion

We have demonstrated non-destructive longitudinal characterization of NANF microstructure, showing measurements of both nested capillary mean diameters along 2.2 km of fiber and also showing how we can introduce and detect twist. The diameter measurements show both good longitudinal resolution and robustness to fiber speed, making this a powerful tool for accurately characterizing NANF, both during and after fabrication. This could reduce the need to cut and view fiber samples during fabrication, leading to the production of longer lengths of highly uniform NANF. Whilst it has previously been possible to infer the twist state of a fiber through backwards propagation of the Jones matrix [8], we here, to the best of our knowledge, show the first in-situ direct measurement of fiber twist.

We acknowledge funding from the ERC (LightPipe, g.a. 682724), UK RAEng, Honeywell Inc. and the U.S. Government under the DoD Ordnance Technology Consortium (DOTC) Other Transaction Agreement (OTA) (W15QKN-18-9-1008).

References

[1] F. Poletti, "Nested antiresonant nodeless hollow core fiber," *Opt. Express* **22** (20), 23807-23828 (2014).
[2] T.D. Bradley et al., "Antiresonant hollow core fibre with 0.65 dB/km attenuation in the C and L telecommunication bands," ECOC 2019, PD.3.1.
[3] H. Sakr et al., "Hollow Core NANFs with Five Nested Tubes and Record Low Loss at 850, 1060, 1300 and 1625nm," OFC 2021, F3A.4.
[4] A. Taranta et al., "Exceptional polarization purity in antiresonant hollow-core optical fibres," *Nat. Photonics* **14** (8), 504-510 (2020).
[5] M.H. Frosz et al., "Non-invasive real-time characterization of hollow-core photonic crystal fibers using whispering gallery mode spectroscopy," *Opt. Express* **27** (21), 30842-30851 (2019).
[6] L. Budd et al., "Non-Invasive Measurement of Hollow-Core Antiresonant Fiber Structure," IEEE IPC 2021, ThG2.2.
[7] L. Budd et al., "Non-Destructive Structural Characterisation of Double Nested Antiresonant Nodeless Fiber," Optica APC 2022, SoTh3G.1.
[8] D. Tentori et al., "Jones birefringence in twisted single-mode optical fibers," *Opt. Express* **21** (26), 31725-31739 (2013).